J Appl Electrochem (2009) 39:421–427
DOI 10.1007/s10800-008-9687-z

ORIGINAL PAPER

Electrochemical behavior of vanadium-substituted Keggin-type polyoxometalates in aqueous solution

Chunxiang Li · Yan Zhang · Kevin P. O'Halloran · Jiawei Zhang · Huiyuan Ma

Received: 16 November 2007 / Accepted: 7 October 2008 / Published online: 5 November 2008

Abstract Cyclic voltammetry was carried out on selected vanadium-substituted Keggin polyoxometalates in aqueous solution with a focus on $K_3H_2[\alpha\text{-}SiVW_{11}O_{40}] \cdot 6H_2O$ ($SiVW_{11}O_{40}$) and $K_4H_2[\gamma(1,2)\text{-}SiV_2W_{10}O_{40}] \cdot 4H_2O$ ($SiV_2W_{10}O_{40}$). The redox waves of the V-O and W-O framework for both polyanions are pH- and scan rate-dependent. The first vanadium-centered wave (V-wave) for $SiVW_{11}O_{40}$ shows a classical potential shift as a function of acidity at pH < 3.5, and then becomes pH-independent above this value. Above pH 3.5, the W-centers in $SiVW_{11}O_{40}$ and $SiV_2W_{10}O_{40}$ exhibit efficient electrocatalytic activity towards the reduction of nitrite and hydrogen peroxide while the V-waves also exhibit an electrocatalytic response in nitrite-containing solutions.

Keywords Electrochemistry · Electrocatalysis · Polyoxometalate · Vanadium-substituted polyoxometalate · $SiVW_{11}$ · SiV_2W_{10}

1 Introduction

Polyoxometalates (POMs) constitute a unique class of molecular, metal-oxygen clusters and are remarkable in several respects: the variety of their properties based on their sizes, shapes, charge densities, and the enormous diversity of their structures [1, 2]. Some polyoxometalates with Keggin or Dawson structures have the ability to participate in multiple, consecutive, and reversible multi-electron reductions without decomposition to mixed-valence species (called heteropolyblues). Therefore, polyoxometalates are good candidates for applications in a wide range of areas including catalysis, electrocatalysis, medicine, materials science, photochemistry, analytical chemistry, and magnetochemistry [3–5].

Polyoxo-tungstates and -molybdates have been extensively studied as electrocatalysts [6, 7]. However, the electrochemical and electrocatalytic properties of the vanadium-substituted polyoxometalates have been much less studied than those of the parent Keggin anions [3, 7–31]. The replacement of W^{VI} (or Mo^{VI}) with V^{V} makes it possible to modify the electrochemical properties of the polyoxometalates [32, 33]. The order of decreasing oxidizing ability is: V(V) > Mo(IV) > W(IV). Moreover, substitution of vanadium into the POM framework can shift the stability of the plenary species to higher pH, which is important in several catalytic and electrocatalytic processes [17, 18, 20, 24–27, 34, 35]. For example, vanadium-substituted POMs can effectively catalyze the oxidation of NADH to NAD^+ above pH 6.8 [7, 36, 37], which is a very important process in biological systems. It is, therefore, of interest to unambiguously identify the nature of the redox processes associated with these versatile, vanadium-substituted Keggin ion derivatives.

With this in mind, we have studied the electrochemical properties of two vanadium-substituted derivatives of Keggin polyoxometalates, $K_3H_2[\alpha\text{-}SiVW_{11}O_{40}] \cdot 6H_2O$ and $K_4H_2[\gamma(1,2)\text{-}SiV_2W_{10}O_{40}] \cdot 4H_2O$, by cyclic voltammetry (CV) in aqueous solutions and their electrocatalytic

C. Li · J. Zhang · H. Ma (✉)
Department of Chemistry, Harbin Normal University, Harbin 150025, People's Republic of China
e-mail: mahy017@163.com

Y. Zhang
College of Life and Environmental Sciences, Central University for Nationalities, Beijing 100081, People's Republic of China

K. P. O'Halloran
Department of Chemistry, Emory University, Atlanta, Georgia 30322, USA

reduction of NO_2^- and H_2O_2. The results provide valuable information of their electrochemical and electrocatalytic properties.

2 Experimental

2.1 Reagents

The preparation of $K_4H_2[\gamma(1, 2)\text{-}SiV_2W_{10}O_{40}] \cdot 4H_2O$ ($SiV_2W_{10}O_{40}$) and $K_3H_2[\alpha\text{-}SiVW_{11}O_{40}] \cdot 6H_2O$ ($SiVW_{11}O_{40}$) have already been described in detail [38, 39]. Buffer solutions were prepared from either 0.5 M CH_3COONa–CH_3COOH (pH 3–6), 0.5 M Na_2SO_4–H_2SO_4 (pH 1–3) or 0.1 M NaH_2PO_4–NaOH (pH $\geq$ 7). All solutions were deaerated with pure nitrogen before use. The water used in all experiments was deionized to a resistivity of 16–18 MΩ cm. All of the chemicals were of high-purity grade and were used without further purification.

2.2 Electrochemical measurements

Cyclic voltammetry was carried out in a three compartment cell (10 mL) with a CHI600 voltammetric analyzer at ambient temperature (20 ± 2 °C). All potentials are given with respect to a commercial Ag/AgCl reference electrode. A twisted platinum wire was used as the counter electrode and a glassy carbon electrode (GCE) as the working electrode. The GCEs were polished with 1.0 and 0.3 μm α-Al_2O_3 powders, and subsequently sonicated in water for about 5 min after each polishing step. Finally, the electrodes were sonicated in ethanol, washed, and then dried in a high purity nitrogen stream immediately before use.

Formal potentials (E_f) of the redox couples in the CVs were estimated as average values of anodic (E_{pa}) and cathodic (E_{pc}) peak potentials, i.e., $E_f = (E_{pa} + E_{pc})/2$; and peak potential separations $\Delta E_p = E_{pa} - E_{pc}$. Perfect reproducibility of the voltammogram for a selected potential scan rate was taken as a complementary stability criterion.

3 Results and discussion

3.1 Electrochemical behavior of $SiVW_{11}O_{40}$ and $SiV_2W_{10}O_{40}$

$SiVW_{11}O_{40}$ and $SiV_2W_{10}O_{40}$ were selected as the representative polyoxometalates because they are considered to display one of the most complete sets of electrochemical behaviors among vanadium-substituted Keggin polyoxometalates. It is well known that the electrochemical behaviors of POMs are affected by solution properties such as acidity. Therefore, CH_3COONa–CH_3COOH buffered solution was selected for W-wave studies while NaH_2PO_4–NaOH solution was selected for V-wave studies.

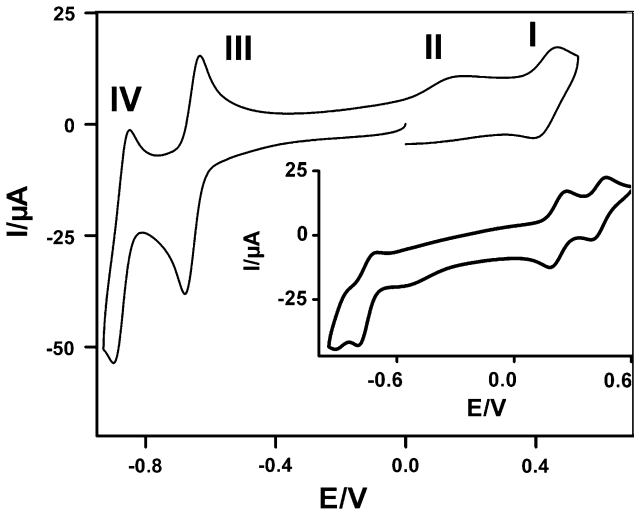

Fig. 1 Cyclic voltammograms (CVs) of 2 mM $SiVW_{11}O_{40}$ at pH 3.84 (0.5 M CH_3COONa–CH_3COOH). Inset the CV of 2 mM $SiVW_{11}O_{40}$ at pH 7 (0.1 M NaH_2PO_4–NaOH) buffer solution. The scan rate was 50 mV s^{-1}, the working electrode was glassy carbon, and the reference electrode was Ag/AgCl electrode

The values of E_f for $SiVW_{11}O_{40}$ by cyclic voltammetry in 0.5 M CH_3COONa–CH_3COOH (pH 3.84) (Fig. 1) are in agreement with voltammetric results of $SiMo_2VW_9$ previously reported [11]. The two sets of clearly defined redox peaks found at −0.656 and −0.875 V (waves III and IV) are attributed to two two-electron, tungsten-centered ($W^{VI} \rightarrow W^{V}$) redox processes, and the other two sets of redox peaks (waves I and II) are assigned to the V-center reductions [40]. The cyclic voltammetric measurements for SiW_{11} V in 0.1 M NaH_2PO_4-NaOH (pH 7) buffer solution (inset Fig. 1), yielded two clearly defined redox peaks centered at 0.428 and 0.147 V, assigned formally to the one-electron vanadium-centered reductions, ($V^{V} \rightarrow V^{IV}$) and ($V^{IV} \rightarrow V^{III}$), respectively, and the two sets of redox peaks found at more negative potentials are attributed to W-based reductions. Comparing the CVs at different pH conditions, it can be seen that waves I and II are largely reversible in 0.1 M NaH_2PO_4–NaOH (pH 7) buffer solutions while wave II is irreversible upon potential reversal in pH 3.84 solutions, demonstrating that the second V-wave is a function of the pH while the first V-wave is not.

As shown in Fig. 2, the $SiV_2W_{10}O_{40}$ exhibits five redox waves with E_f values of 0.295, −0.224, −0.493, −0.614, and −0.727 V in the potential range 0.46 to −0.8 V, which are assigned, respectively, to a one-electron vanadium-centered ($V^{V} \rightarrow V^{IV}$), a one-electron tungsten-centered ($W^{VI} \rightarrow W^{V}$), a two-electron vanadium-centered ($V^{V} \rightarrow V^{III}$), a one-electron tungsten-centered ($W^{VI} \rightarrow W^{V}$), and two one-electron tungsten-centered ($W^{VI} \rightarrow W^{V}$) redox processes of

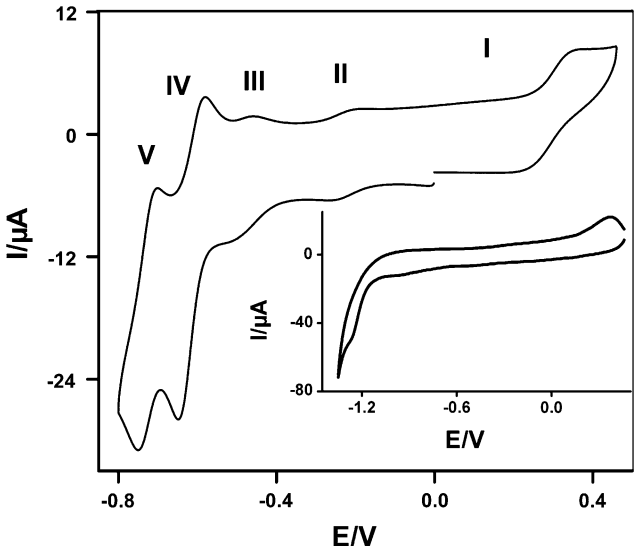

Fig. 2 CVs of 1 mM $SiV_2W_{10}O_{40}$ at pH 4.35 (0.5 M CH_3COONa–CH_3COOH). Inset the CV of 1 mM $SiV_2W_{10}O_{40}$ at pH 7 (0.1 M NaH_2PO_4–NaOH) buffer solution. The scan rate was 30 mV s^{-1}, the working electrode was glassy carbon, and the reference electrode was Ag/AgCl electrode

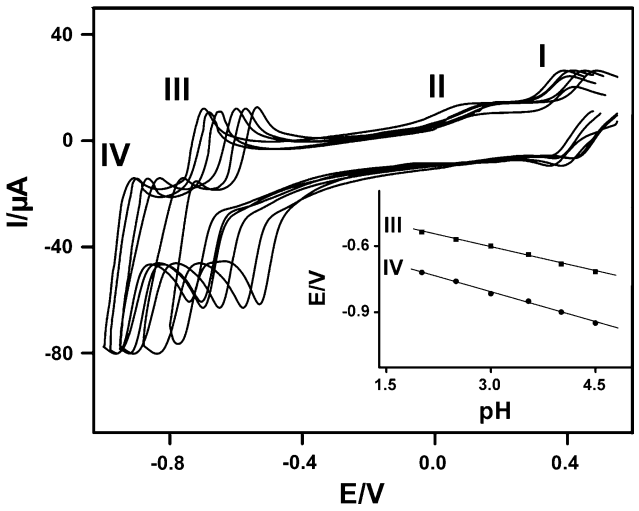

Fig. 3 CVs for 2 mM $SiVW_{11}O_{40}$ in acetate buffer solution at various pH values (from right to left: 2.0, 2.5, 3.0, 3.5, 4.0, 4.5). Scan rate was 50 mV s^{-1}. Inset: the relationship between peak potentials of the third and fourth redox waves versus pH and an enlargement of the V part

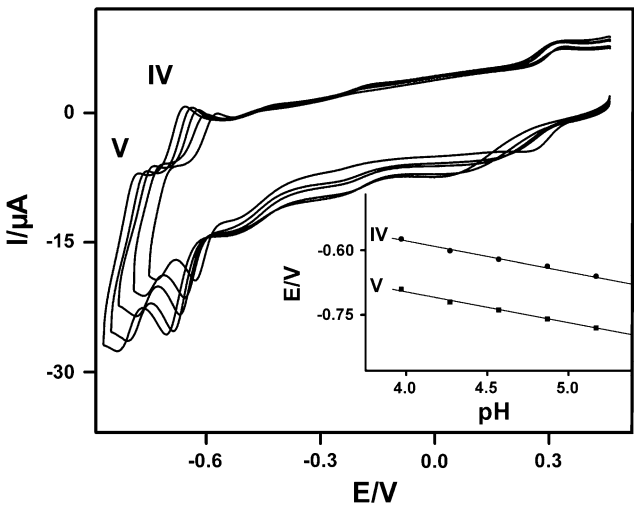

Fig. 4 CVs for 1 mM $SiV_2W_{10}O_{40}$ in acetate buffer solution at various pH values (from right to left: 3.97, 4.27, 4.57, 4.87, and 5.17). Scan rate was 50 mV s^{-1}. Inset: the relationship between peak potentials of the fourth and fifth redox waves versus pH

$SiV_2W_{10}O_{40}$ [15, 31]. Compared to the CV of $SiMoV_2W_9$ reported by Hervé, waves I and II for $SiV_2W_{10}O_{40}$ are positively shifted (ca. 40 mV), while wave III is negatively shifted (ca. 10 mV). In contrast to $SiVW_{11}O_{40}$, the V-waves of $SiV_2W_{10}O_{40}$ are largely irreversible in 0.1 M NaH_2PO_4-NaOH (pH 7) buffer solutions (inset of Fig. 2). The second V-wave of $SiV_2W_{10}O_{40}$ is located at −0.493 V while that of $SiVW_{11}O_{40}$ is located at 0.147 V. This phenomenon may be explained as follows: W-based orbitals are the lowest unoccupied molecular orbitals which are delocalized over the entire polyoxometalate framework. Since the decreasing oxidizing character follows the sequence V > Mo > W, when the number of V atoms in the framework is increased, the added electrons are localized on vanadium [19].

3.2 Effect of pH

In general, the reduction of POMs is accompanied by protonation; therefore, the electrochemical behavior of POMs is pH-dependant to a large extent. Figure 3 gives a detailed picture of the evolution of $SiVW_{11}O_{40}$ as a function of pH. Over the pH range 2.0–4.5 in acetate buffer, four waves move in the positive direction as the pH decreases. The inset of Fig. 3 shows the linear relationship between the corresponding redox potential versus pH with different slopes: 74 mV/pH for wave III and 86 mV/pH for wave IV, which suggest different levels of protonation accompanying these redox reactions. The variation of W-waves with acidity is common in POM electrochemistry. In contrast, it is worth noting that the potential of the first V-wave remained fixed in the pH domain 3.5–4.5. In fact, this pH-independence was observed from approximately pH 3.5 to 7 (inset of Fig. 1). That is to say, in the pH range 2.0–3.5, as the pH increased the potential for the first V-wave shifted negatively. In the pH range 3.5–7, as the pH increased the peak potential for the first V-wave remained unchanged. In contrast, the second V-wave shifted negatively with an increase in pH in the range 3.5–7.

The CVs of $SiV_2W_{10}O_{40}$ in acetate buffer at different pH values are shown in Fig. 4. When the pH increased from 3.97 to 5.17, the redox wave potentials moved negatively and the current increased. A clear evolution in peak

current intensities and peak widths is still observed between pH 3.97 to 5.17. In contrast to the behavior of W-waves, the cathodic potential of wave I stayed almost the same while the anodic wave potential gradually moved negatively in the pH domain 3.97–5.17. As shown in the inset of Fig. 4, the slopes of wave IV and V are 67 mV/pH and 63 mV/pH, respectively, which are close to the theoretical value −60 mV/pH for $2e^-/2H^+$, confirming the addition of two H^+ to the two-electron reduction [41]. The rate of change for $SiV_2W_{10}O_{40}$ at various pH values is nearly the same as that of $SiVW_{11}O_{40}$, albeit for a very slight difference in formal potentials.

3.3 Effect of scan rate

Figure 5a presents the cyclic voltammetric behaviors for $SiVW_{11}O_{40}$ at different scan rates in acetate buffer solution (pH 3.84). It is clearly seen that with variation of scan rate from 20 to 180 mV s^{-1}, the reversible redox peaks currents of waves I, II and III for $SiVW_{11}O_{40}$ increased. The peak potentials for waves III and IV were dependent on scan rate. Moreover, the redox steps of waves III and IV were irreversible while those of waves I and II were reversible because the cathodic peak shifted more negatively and the anodic peak more positively with increasing scan rate. With increase in scan rate, the cathodic wave current of wave IV increased more quickly than that of the counterpart; such behavior implies that an intermediate may exist during reduction wave IV [42]. When the scan rate was gradually increased, the intermediate was quickly reduced and could not be detected. From the current versus scan rate, taking wave III as an example, the slope is 0.135 mA s V^{-1} (anodic), and −0.313 mA s V^{-1} (cathodic) (inset of Fig. 5a). This phenomenon also occurred in CVs of $SiV_2W_{10}O_{40}$ in acetate buffer solutions (pH 4.35) (Fig. 5b). The peak potential separations (ΔE_p) of waves IV and V were dependent on scan rate, and the reduction of waves I, II, and III were reversible. The slopes for wave IV: 0.044 mA s V^{-1} (anodic), −0.16 mA s V^{-1} (cathodic) which occurred due to an intermediate in reduction wave IV (inset of Fig. 5b).

In summary, the electrochemical behavior of the $SiVW_{11}O_{40}$ and $SiV_2W_{10}O_{40}$ can be described by the following equations:

$$SiV^{V}W_{11}{}^{VI}O_{40}{}^{5-} + e \rightleftharpoons SiV^{IV}W_{11}{}^{VI}O_{40}{}^{6-}$$

$$SiV^{IV}W_{11}{}^{VI}O_{40}{}^{6-} + e + H^+ \rightleftharpoons HSiV^{III}W_{11}{}^{VI}O_{40}{}^{6-}$$

$$SiV^{III}W_{11}{}^{VI}O_{40}{}^{6-} + 2H^+ + 2e \rightleftharpoons H_2SiV^{III}W_9{}^{VI}W_2{}^{V}O_{40}{}^{6-}$$

$$H_2SiV^{III}W_9{}^{VI}W_2{}^{V}O_{40}{}^{6-} + 2e + 2H^+ \rightleftharpoons H_4SiV^{III}W_7{}^{VI}W_4{}^{V}O_{40}{}^{6-} \quad (a)$$

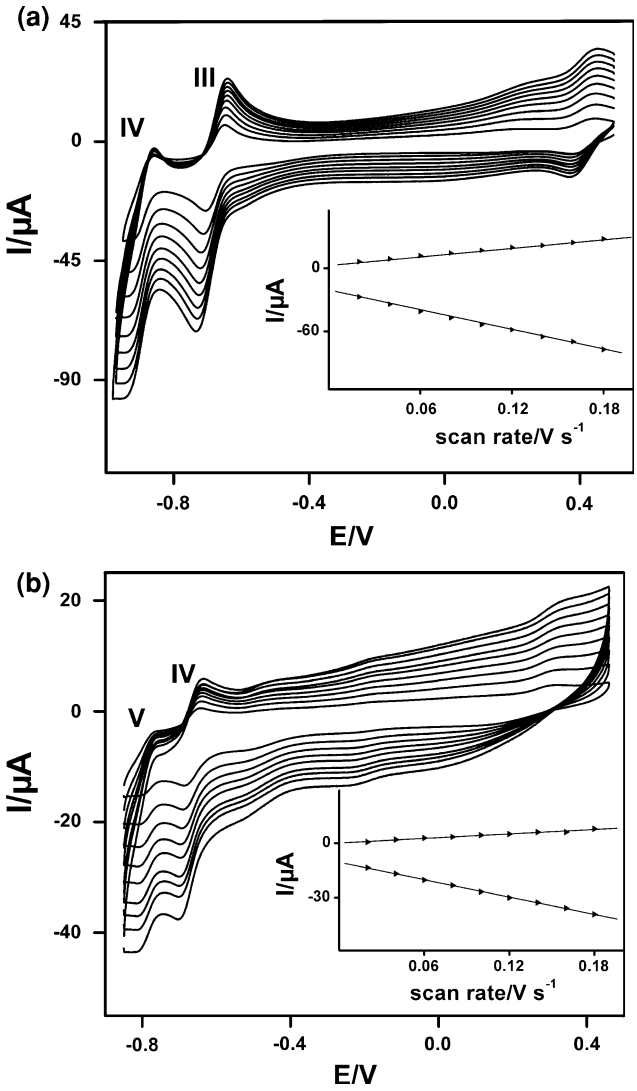

Fig. 5 CVs for $SiVW_{11}O_{40}$ and $SiV_2W_{10}O_{40}$ at different scan rates in 0.5 M CH_3COONa–CH_3COOH media. From inner to outer: 20, 40, 60, 80, 100, 120, 140, and 160, 180 mV s^{-1}. **a** CVs of 2 mM $SiVW_{11}O_{40}$ (pH 3.84). The inset shows plots of the anodic and the cathodic peak currents for wave III versus scan rates. **b** CVs of 2 mM $SiV_2W_{10}O_{40}$ (pH 4.35). The inset shows plots of the anodic and the cathodic peak currents for wave IV versus scan rates

$$SiV_2{}^{V}W_{10}{}^{VI}O_{40}{}^{6-} + e + H^+ \rightleftharpoons HSiV^{IV}V^{V}W_{10}{}^{VI}O_{40}{}^{6-}$$

$$HSiV^{IV}V^{V}W_{10}{}^{VI}O_{40}{}^{6-} + e + H^+ \rightleftharpoons H_2SiV^{IV}V^{V}W_9{}^{VI}W^{V}O_{40}{}^{6-}$$

$$H_2SiV^{IV}V^{V}W_9{}^{VI}W^{V}O_{40}{}^{6-} + 2e + 2H^+ \rightleftharpoons H_4SiV^{IV}V^{III}W_9{}^{VI}W^{V}O_{40}{}^{6-}$$

$$H_4SiV^{IV}V^{III}W_9{}^{VI}W^{V}O_{40}{}^{6-} + e + H^+ \rightleftharpoons H_5SiV^{IV}V^{III}W_8{}^{VI}W_2{}^{V}O_{40}{}^{6-}$$

$$H_5SiV^{IV}V^{III}W_8{}^{VI}W_2{}^{V}O_{40}{}^{6-} + 2e + 2H^+ \rightleftharpoons H_7SiV^{IV}V^{III}W_6{}^{VI}W_4{}^{V}O_{40}{}^{6-} \quad (b)$$

3.4 Electrocatalytic properties

POMs possess a unique set of properties that are extremely valuable for catalysis. They can contain different ratios of Mo^{VI}, W^{VI} and V^{VI} in their frameworks, a variety of elements as central atoms, or ligands. Polyoxometalates are multi-electron oxidants (they can gain as many as six or more electrons without decomposition of the polyanion), and they are also strong Brönsted acids [1]. Redox and acidic properties of POMs can be varied over rather wide ranges by modifying their compositions. Vanadium-substituted $SiV_2W_{10}O_{40}$ and $SiVW_{11}O_{40}$ are highly soluble and fairly stable in water, and they are thermally stable in the solid state which renders them useful as both homogeneous and heterogeneous oxidative and acid catalysts.

Catalytic reduction of the NO_x compounds, particularly nitrite, by reduced vanadium-substituted POMs has become a classical test for their electrocatalytic abilities since the pioneering work in this area [43–48]. General aspects of such electrocatalytic processes were discussed recently [49]. Figure 6a shows the CVs of $SiVW_{11}O_{40}$ containing NO_2^- at various concentrations. The current of the W-centered reduction of wave III and IV at potentials of −0.65 and −0.87 V increased markedly with increasing NO_2^- concentration, while the oxidation peak decreased. This demonstrates that the reduction of NO_2^- is effectively electrocatalyzed by $SiVW_{11}O_{40}$. The insets of Fig. 6a show the linear relationships of catalytic currents of waves III and IV versus concentrations of NO_2^-. Figure 6b shows the cathodic current increase and the anodic current decrease accompanying the addition of NO_2^- to a solution of $SiV_2W_{10}O_{40}$ in acetate buffer at pH 4.57. Clearly, waves IV and V for $SiV_2W_{10}O_{40}$ catalyze the reduction of NO_2^- effectively, and they have higher catalytic activity than waves II and III. The magnitude of current enhancement decreases gradually for waves II and III of $SiV_2W_{10}O_{40}$ indicating lower catalytic activity. However, the cathodic current increase and the anodic current decrease at the second V-center of wave III are easily observed which suggests that the reduction of NO_2^- is effectively electrocatalyzed by the V-center. This behavior is rarely reported in the literature [30].

Figure 7a shows the cyclic voltammograms of $SiVW_{11}O_{40}$ in acetate buffer solution (pH 3.84) in the absence and presence of H_2O_2. The reduction currents of waves III and IV increased, while the oxidation peak decreased for each addition of H_2O_2, demonstrating stable and efficient catalytic activity of the $SiVW_{11}O_{40}$. The electrocatalytic behavior above can be described by the following mechanism:

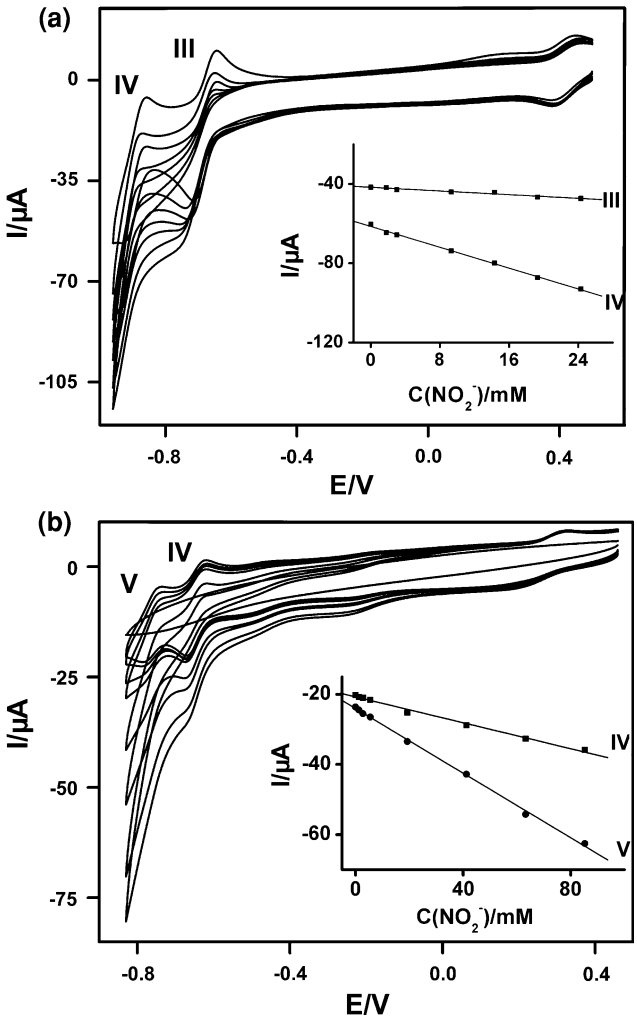

Fig. 6 Reduction of nitrite by $SiVW_{11}O_{40}$ and $SiV_2W_{10}O_{40}$ 0.5 M CH_3COONa–CH_3COOH media containing NO_2^- in various concentrations (upper line: CV of a bare GCE in corresponding buffer solution with 1.25 mM NO_2^-.) Scan rate was 50 mV s^{-1}. **a** CVs of 2 mM $SiVW_{11}O_{40}$ (pH 3.81). The NO_2^- concentrations from top to bottom: 0, 1.8, 3.0, 9.3, 14.3 and 19.3, 24.3 mM. The inset shows relationship between the third and fourth cathodic current and concentration of NO_2^-. **b** CVs of 2 mM $SiV_2W_{10}O_{40}$ (pH 4.57). The NO_2^- concentrations from top to bottom: 0, 1.25, 2.75, 5.5, 19.25, 41.25 and 63.25, 85.25 mM. The inset shows relationship between the fourth and fifth cathodic current and concentration of NO_2^-

$$SiV^{III}W_{11}{}^{VI}O_{40}{}^{6-} + 2H^+ + 2e \rightleftharpoons H_2SiV^{III}W_9{}^{VI}W_2{}^{V}O_{40}{}^{6-}$$

$$H_2SiV^{III}W_9{}^{VI}W_2{}^{V}O_{40}{}^{6-} + 2e + 2H^+ \rightleftharpoons H_4SiV^{III}W_7{}^{VI}W_4{}^{V}O_{40}{}^{6-}$$

$$H_4SiV^{III}W_7{}^{VI}W_4{}^{V}O_{40}{}^{6-} + H_2O_2 \rightleftharpoons H_4SiV^{III}W_7{}^{VI}W_4{}^{V}O_{40}{}^{6-\bullet}H_2O_2$$

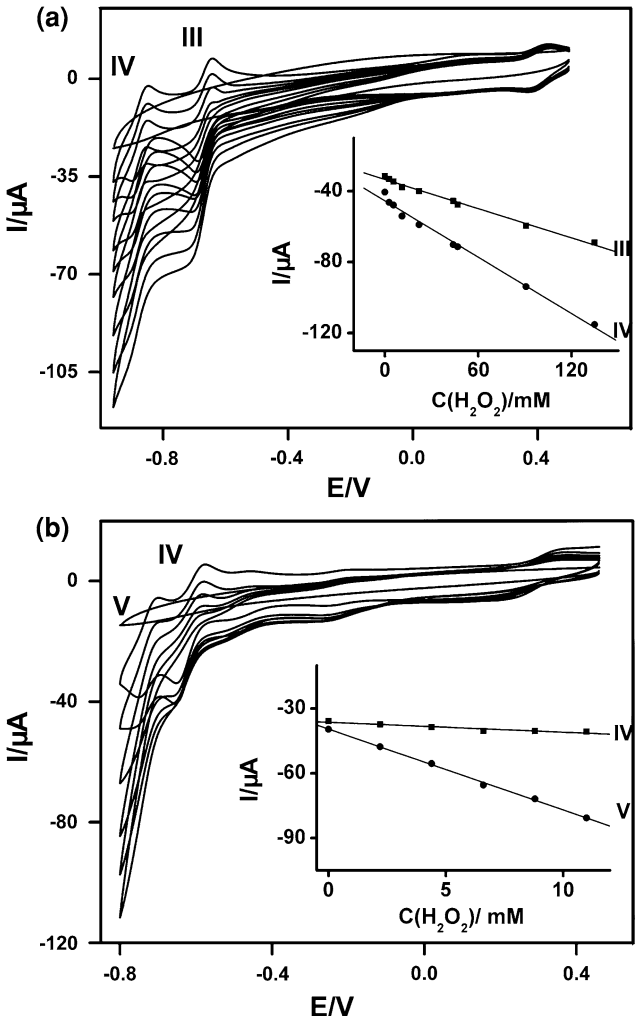

Fig. 7 Reduction of H_2O_2 by $SiVW_{11}O_{40}$ and $SiV_2W_{10}O_{40}$ in 0.5 M CH_3COONa–CH_3COOH media containing H_2O_2 in various concentrations. (upper line: CV of a bare GCE in correspond media with 2.5 mM H_2O_2.) Scan rate was 50 mV s^{-1}. **a** CVs of 2 mM $SiVW_{11}O_{40}$ (pH 3.84). The H_2O_2 concentrations from top to bottom: 0, 2.75, 5.5, 11, 22, 44, 46.75, 90.75 and 134.75, 178.75 mM. The inset shows the relationship between the third and the fourth cathodic current vs. concentration of H_2O_2. **b** CVs of 2 mM $SiV_2W_{10}O_{40}$ (pH 4.35). The H_2O_2 concentrations from top to bottom: 0, 2.2, 4.4, 6.6 and 8.8, 11 mM. The inset shows relationship between the third and fourth cathodic current vs. concentration of H_2O_2

$$H_4SiV^{III}W_7{}^{VI}W_4{}^{V}O_{40}{}^{6-}\bullet H_2O_2 \rightarrow 1/2\ H_2SiV^{III}W_9{}^{VI}W_2{}^{V}O_{40}{}^{6-} + H_2O + 1/2\ H_4SiV^{III}W_7{}^{VI}W_4{}^{V}O_{40}{}^{6-} + OH$$

$$1/2\ H_4SiV^{III}W_7{}^{VI}W_4{}^{V}O_{40}{}^{6-} + OH \rightarrow 1/2\ H_2SiV^{III}W_9{}^{VI}W_2{}^{V}O_{40}{}^{6-} + H_2O$$

The last two steps above can be expressed by

$$H_4SiV^{III}W_7{}^{VI}W_4{}^{V}O_{40}{}^{6-} + H_2O_2 \rightarrow H_2SiV^{III}W_9{}^{VI}W_2{}^{V}O_{40}{}^{6-} + 2H_2O$$

A similar phenomenon was observed for $SiV_2W_{10}O_{40}$: with the addition of hydrogen peroxide, the magnitude of waves IV and V for the cathodic currents of $SiVW_{11}O_{40}$ were significantly increased while the anodic currents were decreased (Fig. 7b), which can be described as:

$$H_7SiV^{IV}V^{III}W_6{}^{VI}W_4{}^{V}O_{40}{}^{6-} + H_2O_2 \rightarrow H_5SiV^{IV}V^{III}W_8{}^{VI}W_2{}^{V}O_{40}{}^{6-} + 2H_2O$$

Compared with $SiVW_{11}O_{40}$, $SiV_2W_{10}O_{40}$ has higher electrocatlytic activity towards the reduction of H_2O_2: the slopes of currents for waves IV and V versus hydrogen peroxide are 0.525 and 3.739, which are much larger than that of $SiVW_{11}O_{40}$ (0.216 and 0.486) (inset of Fig. 7a, b).

4 Conclusion

We have studied the electrochemical properties of $SiVW_{11}O_{40}$ and $SiV_2W_{10}O_{40}$ in aqueous solutions. The selected POMs exhibit good electrochemical and electrocatalytic properties at higher pH values due to the presence of vanadium atoms, which is important to several catalytic and electrocatalytic processes. The redox waves of the V-O and W-O framework are pH- and scan rate-dependent. When the scan rate increased, the reversible redox peak currents of $SiVW_{11}O_{40}$ and $SiV_2W_{10}O_{40}$ increased with different slopes of current versus scan rate for anodic and cathodic peaks (except for the anodic wave current of the last wave for $SiVW_{11}O_{40}$ and $SiV_2W_{10}O_{40}$, which decreased). Additionally, the reduction of NO_2^- and H_2O_2 can be effectively electrocatalyzed by $SiVW_{11}O_{40}$ and $SiV_2W_{10}O_{40}$ in aqueous solution.

Acknowledgments This work was supported by the National Nature Science Foundation of China (No. 20771031), the China Postdoctoral Science Foundation (No. 200503644) and the Foundation of Education Committee of Heilongjiang (No. 11531228).

References

1. Pope MT (1983) Heteropoly and isopoly oxometalates. Springer-Verlag, Berlin
2. Pope MT, Müller A (1991) Angew Chem Int Ed Engl 30:34
3. Pope MT, Müller A (1994) Polyoxometalates: from platonic solids to anti-retroviral activity. Kluwer Academic Publishers, The Netherlands
4. Pope MT, Müller A (2001) Polyoxometalate chemistry: from topology via self-assembly to applications. Kluwer Academic Publishers, The Netherlands
5. Yamase T, Pope MT (2002) Polyoxometalate chemistry for nanocomposite design. Kluwer Academic Publishers, New York
6. Rehder D (1991) Angew Chem Int Ed Engl 30:148
7. Rehder D (2003) Inorg Chem Commun 6:604
8. Crans DC (1993) Mol Eng 3:277
9. Crans DC (1994) Comments Inorg Chem 16:1

10. Crans DC (1994) Comments Inorg Chem 16:35
11. Smith DP, Pope MT (1973) Inorg Chem 12:331
12. Hervé G, Tézé A, Leyrie M (1979) J Coord Chem 9:245
13. Mossoba MM, O'Connor CJ, Pope MT, Sinn E, Hervé G, Tézé A (1980) J Am Chem Soc 102:6864
14. Harmalker SP, Pope MT (1981) J Am Chem Soc 103:7381
15. Harmalker SP, Leparulo MA, Pope MT (1983) J Am Chem Soc 105:4286
16. Abbessi M, Contant R, Thouvenot R, Hervé G (1991) Inorg Chem 30:1695
17. Mialane P, Marrot J, Rivière E, Nebout J, Hervé G (2001) Inorg Chem 40:44
18. Contant R, Thouvenot R (1991) Can J Chem 69:1498
19. Clinton DE, Tryk DA, Bae IT, Urbach FL, Antonio MR, Scherson DA (1996) J Phys Chem 100:18511
20. Ogawa H, Fujinami H, Taya K, Teratani S (1981) J Chem Soc Chem Commun 24:1274
21. Taraban'ko VE, Khozevnikov IV, Matveev KI (1978) Kinet Katal 19:160
22. Davidson SF, Mann BE, Maitlis PM (1984) J Chem Soc Dalton Trans 6:1223
23. Finke RG, Rapko B, Saxton RJ, Domaille PJ (1986) J Am Chem Soc 108:2948
24. Weiner H, Finke RG (1999) J Am Chem Soc 121:9831
25. Nomiya K, Nemoto Y, Hasegawa T, Matsuoka S (2000) J Mol Catal A: Chemi 152:55
26. Lopez X, Bo C, Poblet JM (2002) J Am Chem Soc 124:12574
27. Contant R, Abbessi M, Thouvenot R, Hervé G (2004) Inorg Chem 43:3597
28. Keita B, Contant R, Mialane P, Sècheresse F, Oliveira P, Nadjo L (2006) Electrochem Commun 8:767
29. Keita B, Mbomekalle IM, Nadjo L, Oliveira P, Ranjbari A, Contant R (2005) C R Chimie 8:1057
30. Keita B, Mbomekalle IM, Nadjo L, Haut C (2004) Electrochem Commun 6:978
31. Cadot E, Fournier M, Tézé A, Herve G (1996) Inorg Chem 35:282
32. Jansen RJJ, Vanveldhuizen HM, Schwegler MA, Vanbekkum HRecl (1994) Trav Chim Pays-Bas 113:115
33. Freund MS, Lewis NS (1994) Inorg Chem 33:1638
34. Essaadi K, Keita B, Nadjo L, Contant R (1994) J Electroanal Chem 367:275
35. Khozevnikov IV, Matveev KI (1983) Appl Catal 5:135
36. Keita B, Essaadi K, Nadjo L, Desmadril M (1995) Chem Phys Lett 237:411
37. Keita B, Essaadi K, Nadjo L, Contant R, Justum Y (2002) J Electroanal Chem 404:271
38. Canny J, Thouvenot R, Tézé A, Hervé G, Leparulo-Loftus M, Pope MT (1991) Inorg Chem 30:976
39. Zhu JG, Wang JX, Chen RS (1990) J Inorg Chem 6:204
40. Bard AJ, Faulkner LR (1980) Electrochemical methods. Fundamentals and applications. Wiley, New York
41. Tang ZY, Liu SQ, Wang EK, Dong SJ (2000) Langmuir 16:5806
42. Cui Y, Xu L, Wang WJ, Gao GG, Wang EB (2006) Chinese J Chem 24:316
43. Keita B, Belhouari A, Nadjo L, Contant R (1995) J Electroanal Chem 381:243
44. Zhai SY, Liu JY, Jiang J, Dong SJ (2003) Electroanal 15:1165
45. Toth JE, Anson FC (1989) J Am Chem Soc 111:2444
46. Keita B, Nadjo L, Contant R, Fournier M, Hervé G (1989) French Patent 89:1728
47. Belhouari A, Keita B, Nadjo L, Contant R (1998) New J Chem 22:83
48. Sadakane M, Steckhan E, Hill CL (1998) Chem Rev 98:219
49. Zhang J, Goh J-K, Tan W-T, Bond AM (2006) Inorg Chem 45:3732